

Energy distribution analysis of the wavepacket simulations of CH₄ and CD₄ scattering

R. Milot *, A.P.J. Jansen

Schuit Institute of Catalysis, ST/SKA, Eindhoven University of Technology, P.O. Box 513, NL-5600 MB Eindhoven, The Netherlands

Received 11 November 1999; accepted for publication 3 February 2000

Abstract

The isotope effect in the scattering of methane is studied by wavepacket simulations of oriented CH₄ and CD₄ molecules from a flat surface including all nine internal vibrations. At a translational energy of up to 96 kJ mol⁻¹ we find that the scattering is still predominantly elastic, but less so for CD₄. Energy distribution analysis of the kinetic energy per mode and the potential-energy surface terms, when the molecule hits the surface, are used in combination with vibrational excitations and the corresponding deformation. They indicate that the orientation with three bonds pointing towards the surface is mostly responsible for the isotope effect in methane dissociation. © 2000 Elsevier Science B.V. All rights reserved.

Keywords: Alkanes; Computer simulations; Low index single crystal surfaces; Models of surface chemical reactions

1. Introduction

The dissociation of methane on transition metals is an important reaction in catalysis. It is the rate-limiting step in steam reforming to produce syngas [1]. It is also prototypical for C–H activation in other processes. A large number of molecular-beam experiments in which the dissociation energy was measured as a function of translational energy have been done on this system [2–22]. These experiments have contributed much to our understanding of the mechanism of dissociation. Some of them observed that vibrationally hot CH₄ dissociates more readily than cold CH₄, with the energy in the internal vibrations being about as effective as the translational energy in inducing dissociation [2–8]. A more detailed

assessment of the importance of the internal vibrations could not be made, because of the large number of internal vibrations. A recent molecular-beam experiment with laser excitation of the ν_3 mode succeeded in measuring a dramatic enhancement of the dissociation on an Ni(100) surface; however, it is still much too low to account for the vibrational activation observed in previous studies and indicates that other vibrationally excited modes contribute significantly to the reactivity of thermal samples [22].

Wavepacket simulations are being used more and more to study the dynamics of this kind of molecule–surface reaction. To date, published wavepacket simulations on the methane dissociation reaction on transition metals always treated the methane molecule as a diatomic [23–27]. Besides the C–H bond and molecule–surface distance, a combination of other coordinates were included such as (multiple) rotations and some

* Corresponding author. Fax: +31-40-2455054.

E-mail address: tgakrm@chem.tue.nl (R. Milot)

lattice motion. None of them has looked at the role of the internal vibrations. Various theoretical studies have obtained reaction pathways and barriers for dissociation by density-functional theory (DFT) calculations [28–37,64], but they cannot explain the role of the vibrational modes in the reaction dynamics either.

A nice way to study reaction dynamics is via the use of isotopes. The most recent wavepacket simulation on the dissociation probability of CH₄ and CD₄ showed semiquantitative agreement with the molecular-beam experiments of Ref. [5], except for the isotope effect and the extracted vibrational efficacy [27]. The molecular-beam study with laser excitation of the ν_3 asymmetric stretch mode showed that the incorrect vibrational efficacy is caused by the assumption in the fit procedure that both stretch modes behave identically [22]. One of the possible explanations for the incorrect isotope effect could be the role played by intramolecular vibrations, which are not included.

In a previous paper we reported on wavepacket simulations carried out to determine which and to what extent internal vibrations are important for the dissociation of CH₄ [38]. We were not yet able to simulate the dissociation including all internal vibrations. Instead we simulated the scattering of methane, for which all internal vibrations can be included, and used the results to deduce consequences for the dissociation. We used model potential-energy surfaces (PESs) that were developed with Ni(111) in mind, but our results should hold for other surfaces as well. At a translational energy of up to 96 kJ mol⁻¹ we found that the scattering is almost completely elastic. Vibrational excitations when the molecule hits the surface and the corresponding deformation depend on generic features of the potential-energy surface. In particular, our simulations indicate that for methane to dissociate the interaction of the molecule with the surface should lead to an elongated equilibrium C–H bond length close to the surface.

We have been using the multiconfigurational time-dependent Hartree (MCTDH) method for our wavepacket simulation, because it can deal with a large number of degrees of freedom and with large grids [39,40]. This method has been

applied successfully to gas-phase reactions and reactions at surfaces [41–60].

In this paper we report wavepacket simulations of CD₄ scattering including all internal vibrations for fixed orientations, performed on the same model PESs as in our previous paper [38]. Translational motion parallel to the surface and all rotational motion were neglected. No degrees of freedom of the surface were included. Experiments show that coupling with these degrees of freedom is dependent on the metal surface. For example, the surface temperature effects observed are small on nickel [5], but quite large on platinum [7]. As we are only interested in the role of internal vibrations, we have not included degrees of freedom of the surface to keep the simulations as simple as possible. We discuss the vibrational excitation and deformation of the CD₄ molecule when it hits the surface and compare it with the case for CH₄. Later we look at the energy distribution of the kinetic energy per mode and the potential energy in some terms of the PES with the elongated equilibrium bond length close to the surface for both isotopes. The transfer of translational kinetic energy towards vibrational kinetic energy gives an indication about the dissociation probability, since vibrational kinetic energy helps in overcoming the dissociation barrier. It gives a better idea about which modes are essential to include in a more accurate wavepacket simulation of methane dissociation, as well. After that we discuss the implications of this for dissociation and give a summary with some general conclusions.

2. Computational details

2.1. The potential-energy surfaces

For the scattering of CD₄ we used the same model PESs as we did for CH₄. Since we expressed the PES in mass-weighted coordinates, the parameters in the PESs for CD₄ differ from those for CH₄. We now give an overview of our model PESs and the corresponding parameters for CD₄. The parameters of CH₄ for these PESs were given previously in Ref. [38], where also more detailed

information about our assumptions and contour plots of some cross-sections of the model PESs can be found.

The PESs we used can all be written as

$$V_{\text{total}} = V_{\text{intra}} + V_{\text{surf}}, \quad (1)$$

where V_{intra} is the intramolecular PES and V_{surf} is the repulsive interaction with the surface. For V_{intra} we looked at four different types of PES. Two of the four different PESs include changes in the intra-molecular potential due to interactions with surface in V_{intra} .

2.1.1. A harmonic potential

The first one is completely harmonic. We have used normal-mode coordinates for the internal vibrations, because these are coupled only very weakly. In the harmonic approximation even this coupling is absent so that we can write V_{intra} as

$$V_{\text{intra}} = V_{\text{harm}} = \frac{1}{2} \sum_{i=2}^{10} k_i X_i^2, \quad (2)$$

the summation is over the internal vibrations, X_i are mass-weighted displacement coordinates and k_i are mass-weighted force constants (see Table 1 for definitions and values); X_1 is the mass-weighted overall translation along the surface normal [61]. The force constants have been obtained by fitting them to the experimental vibrational frequencies of CH_4 and CD_4 [62,63].

We have assumed that the repulsive interaction with the surface is only through the deuterium

atoms that point towards the surface. We take the z -axis as the surface normal. In this case the surface PES is given by

$$V_{\text{surf}} = \frac{A}{N_{\text{D}}} \sum_{i=1}^{N_{\text{D}}} e^{-\alpha z_i}, \quad (3)$$

where N_{D} is the number of deuteriums that point towards the surface, $\alpha = 1.0726$ a.u. (atomic units) and $A = 6.4127$ Hartree. These parameters are chosen to give the same repulsion as the PES that was used in an MCTDH wavepacket simulation of CH_4 dissociation [26].

If we write V_{surf} in terms of normal-mode coordinates, then we obtain for one deuterium pointing towards the surface

$$V_{\text{surf}} = A e^{-\alpha_1 X_1} e^{-\alpha_2 X_2} e^{-\alpha_3 X_3} e^{-\alpha_4 X_4}, \quad (4)$$

where A is as above and α values are as given in Table 2. X_2 , X_3 and X_4 all correspond to a_1 modes of the C_{3v} symmetry (see Fig. 1). There is no coupling between the modes X_5 to X_{10} in the V_{surf} part of the PES, which are all e modes of the C_{3v} symmetry.

For two deuteriums we obtain

$$V_{\text{surf}} = A e^{-\alpha_1 X_1} e^{-\alpha_2 X_2} e^{-\alpha_3 X_3} e^{-\alpha_4 X_4} e^{-\alpha_5 X_5} \\ \times \frac{1}{2} [e^{\beta_3 X_7} e^{-\beta_3 X_8} e^{\beta_5 X_9} e^{-\beta_5 X_{10}} \\ + e^{-\beta_3 X_7} e^{\beta_3 X_8} e^{-\beta_5 X_9} e^{\beta_5 X_{10}}], \quad (5)$$

with A again as above, α and β as given in Table 2. X_2 , X_3 , X_4 and X_5 all correspond to a_1 modes of

Table 1

Overview of the relationships between the mass-weighted coordinates X_i , the force constants k_i (in atomic units) for CD_4 , the designation and the symmetry in T_d , C_{3v} and C_{2v}

i	k_i	Designation	T_d	C_{3v}	C_{2v}
1		translation	t_2	a_1	a_1
2	8.897×10^{-5}	ν_1 ; symmetric stretch	a_1	a_1	a_1
3	2.008×10^{-5}	ν_4 ; umbrella	t_2	a_1	a_1
4	1.060×10^{-4}	ν_3 ; asymmetric stretch	t_2	a_1	a_1
5	2.447×10^{-5}	ν_2 ; bending	e	e	a_1
6	2.447×10^{-5}	ν_2 ; bending	e	e	a_2
7	2.008×10^{-5}	ν_4 ; umbrella	t_2	e	b_1
8	2.008×10^{-5}	ν_4 ; umbrella	t_2	e	b_2
9	1.060×10^{-4}	ν_3 ; asymmetric stretch	t_2	e	b_1
10	1.060×10^{-4}	ν_3 ; asymmetric stretch	t_2	e	b_2

Table 2

α and β values (in a.u.) of V_{surf} for CD_4 with one, two or three deuteriums pointing towards the surface [see Eqs. (4), (5) and (6)]

	One deuterium	Two deuteriums	Three deuteriums
α_1	5.617×10^{-3}	5.617×10^{-3}	5.617×10^{-3}
α_2	8.882×10^{-3}	5.128×10^{-3}	2.960×10^{-3}
α_3	4.703×10^{-3}	-4.614×10^{-3}	-7.720×10^{-3}
α_4	-1.353×10^{-2}	-5.103×10^{-3}	-2.295×10^{-3}
α_5		-7.252×10^{-3}	
β_1			4.187×10^{-3}
β_2			7.252×10^{-3}
β_3		4.659×10^{-3}	2.196×10^{-3}
β_4			3.804×10^{-3}
β_5		4.212×10^{-3}	2.295×10^{-3}
β_6			3.439×10^{-3}

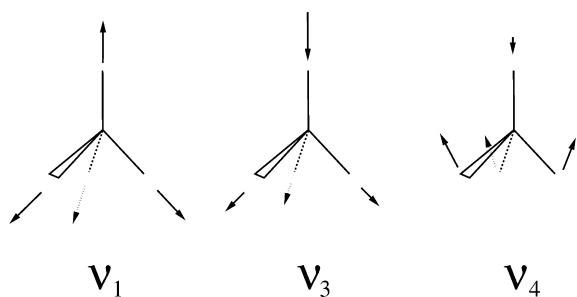


Fig. 1. The a_1 vibrational normal modes in the C_{3v} symmetry: v_1 , symmetric stretch (X_2); v_3 , asymmetric stretch (X_4); and v_4 , umbrella (X_3).

C_{2v} . X_7 , X_8 , X_9 and X_{10} correspond to b_1 and b_2 modes of C_{2v} . X_6 corresponds to the a_2 mode of C_{2v} and has no coupling with the other modes in V_{surf} .

For three deuteriums we obtain

$$V_{\text{surf}} = A e^{-\alpha_1 X_1} e^{-\alpha_2 X_2} e^{-\alpha_3 X_3} e^{-\alpha_4 X_4} \\ \times \frac{1}{3} [e^{\beta_1 X_5} e^{\beta_2 X_6} e^{-\beta_3 X_7} e^{\beta_4 X_8} e^{\beta_5 X_9} e^{-\beta_6 X_{10}} \\ + e^{\beta_1 X_5} e^{-\beta_2 X_6} e^{-\beta_3 X_7} e^{-\beta_4 X_8} e^{\beta_5 X_9} e^{\beta_6 X_{10}} \\ + e^{-2\beta_1 X_5} e^{2\beta_3 X_7} e^{-2\beta_5 X_9}], \quad (6)$$

with A again as above, α and β as given in Table 2. X_2 , X_3 and X_4 correspond to a_1 modes in the C_{3v} symmetry (see Fig. 1). Because these last six coordinates correspond to degenerate e modes of the C_{3v} symmetry, the β parameters are not unique.

2.1.2. An anharmonic intramolecular potential

Even though we do not try to describe the dissociation of methane in this and our previous paper, we do want to determine which internal vibration might be important for this dissociation. The PES should at least allow the molecule to distort partially as when dissociating. The harmonic PES does not do this. Therefore a number of changes have been made. The first is that we describe the C–D bond by a Morse PES,

$$V_{\text{Morse}} = D_e \sum_{i=1}^4 [1 - e^{-\gamma \Delta r_i}]^2, \quad (7)$$

where $D_e = 0.1828$ Hartree (the dissociation energy of methane in the gas phase) and Δr_i is the change

in bond length from the equilibrium distance. γ was calculated by equating the second derivatives along one bond of the harmonic and the Morse PESs. If we transform Eq. (7) back into normal-mode coordinates, we obtain

$$V_{\text{Morse}} = D_e \sum_{i=1}^4 [1 - e^{\gamma_{i2} X_2} e^{\gamma_{i3} X_3} e^{\gamma_{i4} X_4} e^{\gamma_{i7} X_7} \\ \times e^{\gamma_{i8} X_8} e^{\gamma_{i9} X_9} e^{\gamma_{i,10} X_{10}}]^2, \quad (8)$$

with D_e as above. Values of γ are given in Tables 3 and 4. Note that, although we have only changed the PES of the bond lengths, the v_4 umbrella modes are also affected. This is because these modes are not only bending, but also contain some changes of bond length.

The new intramolecular PES now becomes

$$V_{\text{intra}} = V_{\text{harm}} + V_{\text{Morse}} - V_{\text{corr}}, \quad (9)$$

where V_{harm} is as given in Eq. (2) and V_{corr} is the quadratic part of V_{Morse} , which is already in V_{harm} .

2.1.3. Intramolecular potential with weakening C–D bonds

When the methane molecule approaches the surface, the overlap of substrate orbitals and anti-bonding orbitals of the molecule weakens the C–D bonds. We want to include this effect for the C–D bonds of the deuteriums pointing towards the surface. We have redefined the V_{Morse} given in Eq. (8) and also replace it in Eq. (9). A sigmoidal function is used to switch from the gas-phase C–D bond to a bond close to the surface. We have used the following, somewhat arbitrary, approximations. (1) The point of inflection should be at a reasonable distance from the surface. It is set to the turnaround point for a rigid methane molecule with translational energy of 93.2 kJ mol^{-1} plus twice the fall-off distance of the interaction with the surface. (2) The depth of the PES of the C–D bond is 480 kJ mol^{-1} in the gas phase, but only 93.2 kJ mol^{-1} near the surface. The value 93.2 kJ mol^{-1} corresponds to the height of the activation barrier used in our dissociation [26]. (3) The exponential factor is the same as for the interaction with the surface.

If we transform to normal-mode coordinates

Table 3

 γ values (in a.u.) of V_{Morse} for CD_4 with one and three deuteriums pointing towards the surface [see Eq. (8)]

One deuterium	Three deuteriums	Value (a.u.)
$\gamma_{12}, \gamma_{22}, \gamma_{32}, \gamma_{42}$	$\gamma_{12}, \gamma_{22}, \gamma_{32}, \gamma_{42}$	7.629×10^{-3}
$\gamma_{13}, -3\gamma_{23}, -3\gamma_{33}, -3\gamma_{43}$	$-\gamma_{13}, 3\gamma_{23}, 3\gamma_{33}, 3\gamma_{43}$	1.397×10^{-3}
$\gamma_{14}, -3\gamma_{24}, -3\gamma_{34}, -3\gamma_{44}$	$-\gamma_{14}, 3\gamma_{24}, 3\gamma_{34}, 3\gamma_{44}$	-1.454×10^{-2}
$\gamma_{17}, \gamma_{18}, \gamma_{19}, \gamma_{1,10}, \gamma_{28}, \gamma_{2,10}$	$\gamma_{17}, \gamma_{18}, \gamma_{19}, \gamma_{1,10}, \gamma_{28}, \gamma_{2,10}$	0.0
$\gamma_{27}, -2\gamma_{37}, -2\gamma_{47}$	$-\gamma_{27}, 2\gamma_{37}, 2\gamma_{47}$	1.318×10^{-3}
$\gamma_{38}, -\gamma_{48}$	$\gamma_{38}, -\gamma_{48}$	-1.114×10^{-3}
$\gamma_{29}, -2\gamma_{39}, -2\gamma_{49}$	$-\gamma_{29}, 2\gamma_{39}, 2\gamma_{49}$	-1.371×10^{-2}
$\gamma_{3,10}, -\gamma_{4,10}$	$-\gamma_{3,10}, \gamma_{4,10}$	1.187×10^{-2}

Table 4

 γ values (in a.u.) of V_{Morse} for CD_4 with two deuteriums pointing towards the surface [see Eq. (8)]

Two deuteriums	Value (a.u.)
$\gamma_{12}, \gamma_{22}, \gamma_{32}, \gamma_{42}$	7.629×10^{-3}
$\gamma_{13}, \gamma_{23}, -\gamma_{33}, -\gamma_{43}, \gamma_{17}, -\gamma_{27}, \gamma_{37}, -\gamma_{47}, \gamma_{18}, -\gamma_{28}, -\gamma_{38}, \gamma_{48}$	-8.070×10^{-4}
$\gamma_{14}, \gamma_{24}, -\gamma_{34}, -\gamma_{44}, \gamma_{19}, -\gamma_{29}, \gamma_{39}, -\gamma_{49}, \gamma_{1,10}, -\gamma_{2,10}, -\gamma_{3,10}, \gamma_{4,10}$	8.396×10^{-3}

for the particular orientations, we then obtain

$$V_{\text{weak}} = D_e \sum_{i=1}^4 W_i [1 - e^{\gamma_{i2}X_2} e^{\gamma_{i3}X_3} e^{\gamma_{i4}X_4} e^{\gamma_{i7}X_7} \times e^{\gamma_{i8}X_8} e^{\gamma_{i9}X_9} e^{\gamma_{i,10}X_{10}}]^2, \quad (10)$$

where $W_i = 1$ for non-interacting bonds and

$$W_i = \frac{1 + \Omega e^{-\alpha_1 X_1 + \omega}}{1 + e^{-\alpha_1 X_1 + \omega}} \quad (11)$$

for the interacting bonds pointing towards the surface. α_1 is as given in Table 2, γ_s are given in Tables 3 and 4, $\Omega = 1.942 \times 10^{-1}$ and $\omega = 7.197$.

2.1.4. Intramolecular potential with elongation of the C–D bonds

A weakened bond generally not only has a reduced bond strength, but also an increased bond length. We include the effect of the elongation of the C–D bond length of the deuteriums that point towards the surface due to interactions with the surface. We have redefined the V_{Morse} given in Eq. (8) and also replace it in Eq. (9) for this type of PES. We have used the following approximations. (1) The transition state, as determined by Refs. [30,64], has a C–H bond that is 0.54 Å longer

than normal. This elongation should occur at the turn-around point for a rigid methane molecule with a translational energy of 93.2 kJ mol⁻¹. (2) The exponential factor is again the same as for the interaction with the surface.

If we transform to normal-mode coordinates for the particular orientations, then we obtain

$$V_{\text{shift}} = D_e \sum_{i=1}^4 [1 - e^{\gamma_{i2}X_2} e^{\gamma_{i3}X_3} e^{\gamma_{i4}X_4} e^{\gamma_{i7}X_7} e^{\gamma_{i8}X_8} \times e^{\gamma_{i9}X_9} e^{\gamma_{i,10}X_{10}} \exp(S_i e^{-\alpha_1 X_1})]^2, \quad (12)$$

where α_1 is as given in Table 2, γ_s are given in Tables 3 and 4. For the orientation with one deuterium towards the surface we obtain: $S_1 = 2.942 \times 10^2$ and $S_2 = S_3 = S_4 = 0$; with two deuteriums: $S_1 = S_2 = 0$ and $S_3 = S_4 = 1.698 \times 10^2$; and with three deuteriums: $S_1 = 0$ and $S_2 = S_3 = S_4 = 2.942 \times 10^2$.

2.2. Initial states

The exact wavefunction of a D -dimensional system is expressed in the MCTDH approximation

by the form

$$\begin{aligned} \Psi_{\text{MCTDH}}(q_1, \dots, q_D; t) \\ = \sum_{n_1 \dots n_D} c_{n_1 \dots n_D}(t) \psi_{n_1}^{(1)}(q_1; t) \dots \psi_{n_D}^{(D)}(q_D; t). \end{aligned} \quad (13)$$

All initial states in the simulations start with the vibrational ground state. The initial translational part $\psi^{(\text{tr})}$ is represented by a Gaussian wavepacket,

$$\psi^{(\text{tr})}(X_1) = (2\pi\sigma^2)^{-1/4} \exp\left[-\frac{(X_1 - X_0)^2}{2\sigma^2} + iP_1 X_1\right], \quad (14)$$

where σ is the width of the wavepacket (we used $\sigma = 320.248$ a.u.), X_0 is the initial position (we used $X_0 = 11\sigma$, which is far enough from the surface to observe no repulsion) and P_1 is the initial momentum. Since we used mass-weighted coordinates the Gaussian wavepackets are identical for CD_4 and CH_4 . We performed simulations in the energy range of 32 to 96 kJ mol⁻¹. We present here only the results of 96 kJ mol⁻¹ (equivalent to $P_1 = -0.2704$ a.u.), because they showed the most obvious excitation probabilities for V_{Morse} . We used seven natural single-particle states, 512 grid points and a grid length of 15σ for the translational coordinate. With this grid width we can perform simulations with a translational energy up to 144 kJ mol⁻¹.

Gauss–Hermite discrete-variable representations (DVR) [65] were used to represent the wavepackets of the vibrational modes. For all simulations of CD_4 we used the same number of DVR points as for CH_4 , which was five DVR points for the ν_2 bending modes and eight DVR points for the ν_4 umbrella, ν_3 asymmetric stretch and ν_1 symmetric stretch mode for an numerical exact integration, except for the simulations with V_{shift} , where we used 16 DVR points for the ν_1 symmetric stretch mode because of the change in the equilibrium position.

Also, the same configurational basis was used for both isotopes. We did the simulation with one bond pointing towards the surface in eight dimensions, because the ν_2 bending modes X_5 and X_6 do not couple with the other modes. We needed four natural single-particle states for modes X_2 , X_3 and X_4 , and just one for the others. So the number of

configurations was $7^1 \times 4^3 \times 1^4 = 448$. The simulation with two bonds pointing towards the surface was performed in nine dimensions. One of the ν_2 bending modes (X_6) does not couple with the other modes, but for the other mode (X_5) we needed four natural single-particle states. The number of configurations was $7^1 \times 4^4 \times 1^4 = 1792$, because we needed the same number of natural single-particle states as mentioned above for the other modes. We needed 10 dimensions to perform the simulation with three bonds pointing towards the surface. We used here one natural single-particle state for the modes X_5 to X_{10} and four natural single-particle states for X_2 to X_4 , which gave us $7^1 \times 4^3 \times 1^6 = 448$ configurations.

3. Results and discussion

3.1. Excitation probabilities and structure deformation of CD_4

The scattering probabilities for CD_4 are predominantly elastic, as we also found in our previous simulations of CH_4 scattering [38]. The elastic scattering probability is larger than 0.99 for all orientation of the PESs with V_{Morse} and V_{weak} at a translational energy of 96 kJ mol⁻¹. For the PES with V_{shift} we observe an elastic scattering probability of 0.981 for the orientation with one, 0.955 with two and 0.892 with three deuteriums pointing towards the surface. This is lower than we have found for CH_4 , which is 0.956 for the orientation with three hydrogens pointing towards the surface and larger than 0.99 for the others. The higher inelastic scattering probabilities of CD_4 was expected, because the force constants k_i of CD_4 are decreased by up to 50% with respect to those of CH_4 and the translational surface repulsion fall-off differs only little.

When we look at the excitation probabilities at the surface for the PES with V_{Morse} and V_{weak} , then we observe generally an increase for CD_4 compared with CH_4 , except for the ν_4 umbrella mode in the orientation with two bonds pointing towards the surface. Relevant differences in the structure deformations are observed only in the bond angles, which are increased for CD_4 in the orientations

with one and three bonds pointing towards the surface. The deformation of the angle between the bonds pointing towards the surface in the orientation with two bonds pointing towards the surface is decreased for CD_4 . We observe again that the PES with V_{weak} gives larger structure deformations than the PES with V_{Morse} , but the differences are smaller for CD_4 than for CH_4 .

For the PES with V_{shift} we do not observe this effect on the bond-angle deformation. The bond-angle deformation for the orientation with two and three deuteriums pointing towards the surface is the same as for CH_4 , and it is just 0.1° less for the bond angle at the surface side in the orientation with one deuterium pointing towards the surface. The excitation probabilities (see Table 5) for the ν_2 bending and ν_4 umbrella modes become higher for all orientations for CD_4 , which is necessary for getting the same bond-angle deformations as for CH_4 .

The changes in the bond distance for the orientations with one and two bonds pointing towards the surface are almost the same for CD_4 as for CH_4 . For the orientation with three bonds pointing towards the surface, we found that the maximum lengthening of the bonds on the surface side was 0.032 \AA less for CD_4 than for CH_4 . We also found that the shortening of the bond pointing away from the surface is 0.010 \AA more for CD_4 . These are only minimal differences, which also suggest that the bond deformation for CD_4 has been influenced slightly more by the ν_3 asymmetric stretch mode than by the ν_1 symmetric stretch mode. The observed excitation probabilities for these modes do not contradict this, but are not reliable enough for hard conclusions because of their high magnitude. It is also not clear, besides

this problem, what they really represent. Is the excitation caused by a different equilibrium position of the PES at the surface in a mode or is it caused by extra energy in this mode? To answer these questions we decided to do an energy distribution analysis during the scattering for both isotopes.

3.2. Energy distribution in CH_4 and CD_4

The energy distribution analysis was performed by calculating the expectation values of the important term of the Hamiltonian H for the wavefunction $\Psi(t)$ at a certain time t during the scattering of CD_4 and CH_4 for all orientations presented in this and our previous paper [38]. We present here only the results of the PES with V_{shift} , because it is the only model PES for which the energy distribution analysis is relevant for discussion of the dissociation hypotheses later on.

We can obtain good information about the energy distribution per mode by looking at the kinetic energy expectation values $\langle \Psi(t) | T_j | \Psi(t) \rangle$ per mode j (see Table 6), because the kinetic energy operators T_j have no cross terms like the PESs do. When we discuss the kinetic energy of a mode we normally refer to the a_1 mode of the C_{3v} or C_{2v} symmetry, because in these modes we have observed the highest excitation probabilities and the change in kinetic energy in the other modes is generally small.

By looking at the expectation values of some terms of the PES $\langle \Psi(t) | V_{\text{term}} | \Psi(t) \rangle$ (see Table 7), we obtain information about how the kinetics of the scattering is driven by the PES. The V_{surf} PES [see Eqs. (4), (5) and (6)] is the surface hydrogen/deuterium repulsion for a given orienta-

Table 5

Excitation probabilities at the surface, at an initial translational energy of 96 kJ mol^{-1} and all initial vibrational states in the ground state, for the intramolecular PES with elongation of the C–D bonds [see Eq. (12)] in the a_1 modes of the C_{3v} and C_{2v} symmetry, with one, two or three deuteriums pointing towards the surface. These modes are a $\nu_1(a_1)$ symmetrical stretch, a $\nu_2(e)$ bending, a $\nu_3(t_2)$ asymmetrical stretch, and a $\nu_4(t_2)$ umbrella. The irreducible representation in T_d symmetry is given in parentheses

Orientation	$\nu_1(a_1)$ stretch	$\nu_2(e)$ bending	$\nu_3(t_2)$ stretch	$\nu_4(t_2)$ umbrella
One deuterium	0.460		0.910	0.174
Two deuteriums	0.792	0.092	0.830	0.495
Three deuteriums	0.868		0.756	0.387

Table 6

Expectation values of the kinetic energy per mode in mHartree for CH₄ and CD₄, at an initial translational energy of 96 kJ mol⁻¹ and all initial vibrational states in the ground state, for the intramolecular PES with elongation of the C–H/D bonds [see Eq. (12)] in the *a*₁ modes of the *C*_{3v} and *C*_{2v} symmetry, with one, two or three deuteriums/hydrogens pointing towards the surface. These modes are a *v*₁(*a*₁) symmetrical stretch, a *v*₂(*e*) bending, a *v*₃(*t*₂) asymmetrical stretch, and a *v*₄(*t*₂) umbrella. The irreducible representation in *T*_d symmetry is given in parentheses

Isotope	Orientation	Translation	<i>v</i> ₁ (<i>a</i> ₁) stretch	<i>v</i> ₂ (<i>e</i>) bending	<i>v</i> ₃ (<i>t</i> ₂) stretch	<i>v</i> ₄ (<i>t</i> ₂) umbrella
CH ₄	Initial	36.57	3.30	1.75	3.39	1.50
	One hydrogen	16.76	3.56		4.53	1.51
	Two hydrogens	14.59	3.50	1.79	4.67	1.57
	Three hydrogens	20.53	5.32		4.39	1.58
CD ₄	Initial	36.57	2.33	1.24	2.52	1.12
	One deuterium	16.17	2.61		4.09	1.18
	Two deuteriums	14.00	2.78	1.27	4.05	1.27
	Three deuteriums	20.06	4.37		3.80	1.28

Table 7

Expectation values of the potential energy terms in mHartree for CH₄ and CD₄, at an initial translational energy of 96 kJ mol⁻¹ and all initial vibrational states in the ground state, for the intramolecular PES with elongation of the C–H/D bonds [see Eq. (12)]. *V*_{surf} is the total surface–hydrogen/deuterium repulsion; *V*_{harm}(*v*₂) and *V*_{harm}(*v*₄) are the harmonic terms of the intramolecular PES of the *a*₁ modes in the *C*_{3v} and *C*_{2v} symmetry corresponding to a *v*₂(*e*) bending and *v*₄(*t*₂) umbrella modes respectively in the *T*_d symmetry. *V*_{bond}(*R*_{up}) and *V*_{bond}(*R*_{down}) are the potential energy in a single C–H/D bond pointing respectively towards and away from the surface

Isotope	Orientation	<i>V</i> _{surf}	<i>V</i> _{harm} (<i>v</i> ₂)	<i>V</i> _{harm} (<i>v</i> ₄)	<i>V</i> _{bond} (<i>R</i> _{up})	<i>V</i> _{bond} (<i>R</i> _{down})
CH ₄	Initial	0.00	1.75	1.50	3.39	3.39
	One hydrogen	18.20		1.87	3.25	3.85
	Two hydrogens	18.55	2.18	4.01	2.75	3.45
	Three hydrogens	9.22		2.94	3.00	3.74
CD ₄	Initial	0.00	1.24	1.12	2.48	2.48
	One deuterium	17.94		1.89	2.43	3.44
	Two deuteriums	18.45	1.68	4.52	2.29	2.74
	Three deuteriums	8.71		3.49	2.28	3.21

tion. *V*_{harm}(*v*₂) and *V*_{harm}(*v*₄) [see Eq. (2)] are the pure harmonic terms of the intramolecular PES of the *a*₁ modes in the *C*_{3v} and *C*_{2v} symmetry corresponding to *v*₂ bending and *v*₄ umbrella modes, respectively. The pure harmonic correction terms of *V*_{corr} [see Eq. (9)] are included in them. *V*_{bond}(*R*_{up}) and *V*_{bond}(*R*_{down}) are the potential energy in a single C–H or C–D bond pointing respectively towards and away from the surface, and they give the expectation value of one bond term of *V*_{shift} [see Eq. (12)]. All given expectation values are the maximum deviation of the initial values, which effectively means the values at the moment the molecule hits the surface.

The largest changes in expectation values are, of course, in the kinetic energy of the translational

mode. The translational kinetic energy does not become zero as we should expect in classical dynamics. The loss of translational kinetic energy is primary absorbed by the *V*_{surf} terms of the PESs. The expectation values of the *V*_{surf} terms show the ability of the hydrogens or deuteriums to come close to the metal surface, since in real space their exponential fall-offs are the same for both isotopes. For a rigid molecule the sum of the translational kinetic energy and *V*_{surf} should be constant, so all deviations of this sum have to be found back in the intramolecular kinetic energy and other PES terms.

We observe that both the minimum in the translational kinetic energy and the maximum in the *V*_{surf} terms are higher for CH₄ than CD₄, so

we have to find a greater increase in energy in the intramolecular modes and PES terms for CD_4 than for CH_4 . We indeed do so and that can be one of the reasons why we found higher inelastic scatter probabilities for CD_4 for the PES with V_{shift} .

For the orientations with one and two bonds pointing towards the surface we observe a large increase of the kinetic energy in the ν_3 asymmetric stretch mode. If we compare this with the excitation probabilities, we find that the kinetic energy analysis gives indeed a different view on the dynamics. For the orientation with two bonds pointing towards the surface we have found for both isotopes very high excitation probabilities in the ν_1 and ν_3 stretch modes. We know now from the kinetic-energy distribution that, for the ν_1 symmetric stretch mode, the high excitation probability is caused by the change of the equilibrium position of the ν_1 mode in the PES and that, for the ν_3 stretch mode, probably the PES also has become narrower.

For the orientation with three bonds pointing towards the surface we also obtain a large increase of the kinetic energy of the ν_3 asymmetrical stretch mode, but we also find an even larger increase in the kinetic energy of the ν_1 symmetrical stretch mode. The total kinetic energy was extremely large, because the kinetic energy of the translational mode also becomes much larger than for the other orientations. Because of this the V_{surf} terms had to be around twice as low as for the other orientations.

All $V_{\text{bond}}(R_{\text{up}})$ terms become lower compared with the initial value, especially in the orientation with two bonds pointing towards the surface. In the orientation with one bond pointing towards the surface, the $V_{\text{bond}}(R_{\text{down}})$ term became higher. This is caused by the repulsion of V_{surf} in the direction of the bond. The increase of this PES term value is higher for CD_4 than for CH_4 .

In the orientation with three bonds pointing towards the surface we also observe a higher $V_{\text{bond}}(R_{\text{down}})$ value, with also the highest increase for CD_4 . In relation with the somewhat shorter bond distance for R_{down} of CD_4 compared with CH_4 , which was also a bit lower compared with the other orientations, we know now that the hydrogens and especially the deuterium have prob-

lems in following the minimum-energy path of the PES with V_{shift} during the scattering dynamics. This leads to higher kinetic energy in the vibrational modes, which results in more inelastic scattering.

The $V_{\text{harm}}(\nu_2)$ term increases with respect to the initial value, but not as much as the increase of $V_{\text{harm}}(\nu_4)$ for the orientation with two bonds pointing towards the surface. The values of $V_{\text{harm}}(\nu_4)$ for CD_4 are even higher than for CH_4 . We observe also a larger increase of the kinetic energy in the ν_4 umbrella mode for CD_4 than for CH_4 . So although there is somewhat more energy transferred to the vibrational modes for CD_4 than CH_4 , this extra vibrational energy is absorbed especially in the ν_4 umbrella mode of CD_4 .

3.3. Dissociation hypotheses

We wish now to discuss some possible implications of the scattering simulation for the isotope effect on the dissociation of methane. In our previous paper we have already drawn some conclusions about the possible reaction mechanism and which potential type would be necessary for dissociation [38]. We found the direct breaking of a single C–H bond in the initial collision more reasonable than the splats model with a single bond breaking after intermediary Ni–C bond formation as suggested by Ref. [4], because the bond-angle deformation seems too small to allow an Ni–C bond to form. From the simulations with CD_4 we can draw the same conclusions. The PES with V_{shift} gives the same bond-angle deformations for both isotopes, which is not sufficient for the splats model. The other potentials give higher bond-angle deformations for the orientation with three deuteriums pointing towards the surface. If the Ni–C bond formation were to go along this reaction path, then the dissociation of CD_4 should be even more preferable than CH_4 , which is not the case. So we only have to discuss the implication of the scattering simulation for the dissociation probabilities of CH_4 and CD_4 for a reaction mechanism involving direct breaking of a single bond. This reaction mechanism can be influenced by what we call a direct or an indirect effect.

A direct effect is the expected change in the

dissociation probability between CH_4 and CD_4 for a given orientation. Since we expect that we need for dissociation a PES with an elongation of the bonds pointing towards the surface, we only have to look at the isotope effect in the simulation for the PES with V_{shift} for different orientations to discuss some direct effect. It is clear from our simulations that the bond lengthening of CD_4 is smaller than that of CH_4 for the orientation with three bonds pointing towards the surface. If this orientation has a high contribution to the dissociation of methane, then this can be the reason for the higher dissociation probability of CH_4 . In this case our simulations also explain why Ref.[27] did not observe a high enough isotope effect in the dissociation probability of their simulation with CH_4 and CD_4 modelled by a diatomic, because we do not observe a change in bond lengthening between the isotopes for the orientation with one bond pointing towards the surface.

The orientation with three bonds pointing towards the surface is also the orientation with the highest increase of the total vibrational kinetic energy for the PES with V_{shift} , because the energy distribution analysis shows — besides a high increase of the kinetic energy in the ν_3 asymmetric stretch mode — also an high increase in the ν_1 symmetric stretch mode. Since vibrational kinetic energy can be used effectively to overcome the dissociation barrier, the orientation with three bonds is indicated to be a more preferable orientation for dissociation. Moreover, the relative difference in kinetic energy between both isotopes is larger for the ν_1 stretch mode than for the ν_3 stretch mode. If the kinetic energy in the ν_1 stretch mode contributes significantly to overcoming the dissociation barrier, then it is another explanation for the low isotope effect in Ref. [27].

An indirect effect is the expected change in the dissociation probability between CH_4 and CD_4 through changes in the orientation distribution caused by the isotope effect in the vibrational modes. This can be the case if the favourable orientation for dissociation is not near the orientation with three bonds pointing towards the surface, but more in a region where one or two bonds point towards the surface. These orientations do not show a large difference in deformation for the

PES with V_{shift} . We cannot draw an immediate conclusion about the indirect effect from our simulations, since we did not include rotational motion, but our simulations show that an indirect isotope effect can exist. For the PES with V_{Morse} in the orientation with three bonds pointing towards the surface, we observe that CD_4 is able to come closer to the surface than CH_4 . So this rotational orientation should be more preferable for CD_4 than for CH_4 . On the other hand, if the PES in this orientation is more like V_{shift} , the dissociation probability in other orientations can be decreased for CD_4 through a higher probability in inelastic scattering channels.

So, for both effects, the behaviour of the orientation with three bonds pointing towards the surface seems to be essential for a reasonable description of the dissociation mechanism of methane. A wavepacket simulation of methane scattering including one or more rotational degrees of freedom and the vibrational stretch modes will be a good starting model to study the direct and indirect effects, since most of the kinetic energy changes are observed in the stretch modes and so the bending and umbrella modes are only relevant with accurate PESs. Eventually dissociation paths can be introduced in the PES along one or more bonds.

Besides our descriptions of the possible isotope effect for the dissociation extracted from the scatter simulations, we have to keep in mind also that a tunneling mechanism can be responsible for the higher isotope effect observed in the experiment and that a different dissociation barrier in the simulations can enhance this effect of tunneling.

4. Conclusions

The scattering is in all cases predominantly elastic. However, the observed inelastic scattering is higher for CD_4 compared with a previous simulation on CH_4 for the PES with an elongated equilibrium bond length close to the surface. When the molecule hits the surface, we observe in general a higher vibrational excitation for CD_4 than for CH_4 . The PES with an elongated equilibrium bond length close to the surface gives for both isotopes

almost the same deformations, although we observe a somewhat smaller bond lengthening for CD₄ in the orientation with three bonds pointing towards the surface. The other model PESs show differences in the bond-angle deformations and in the distribution of the excitation probabilities of CD₄ and CH₄, especially for the PES with only an anharmonic intramolecular potential.

Energy distribution analysis contributes new information on the scattering dynamics. A higher transfer of translational energy towards vibrational kinetic energy at the surface results in higher inelastic scattering. The highest increase of vibrational kinetic energy is found in the ν_3 asymmetric stretch modes for all orientations and also in the ν_1 symmetric stretch mode for the orientation with three bonds pointing towards the surface, when the PES has an elongated equilibrium bond length close to the surface.

Our simulations give an indication that the isotope effect in methane dissociation is caused mostly by the difference in scattering behaviour of the molecule in the orientation with three bonds pointing towards the surface. At least, multiple vibrational stretch modes should be included for a reasonable description of the isotope effect in the methane dissociation reaction.

Acknowledgements

This research was supported financially by the Council for Chemical Sciences of the Netherlands Organization for Scientific Research (CW-NWO). This work was performed under the auspices of NIOK, the Netherlands Institute for Catalysis Research, Lab Report No. TUE-99-5-02.

References

- [1] J.P. Van Hook, Catal. Rev. Sci. Eng. 21 (1980) 1.
- [2] C.T. Rettner, H.E. Pfnür, D.J. Auerbach, Phys. Rev. Lett. 54 (1985) 2716.
- [3] C.T. Rettner, H.E. Pfnür, D.J. Auerbach, J. Chem. Phys. 84 (1986) 4163.
- [4] M.B. Lee, Q.Y. Yang, S.T. Ceyer, J. Chem. Phys. 87 (1987) 2724.
- [5] P.M. Holmbad, J. Wambach, I. Chorkendorff, J. Chem. Phys. 102 (1995) 8255.
- [6] J.H. Larsen, P.M. Holmblad, I. Chorkendorff, J. Chem. Phys. 110 (1999) 2637.
- [7] A.C. Luntz, D.S. Bethune, J. Chem. Phys. 90 (1989) 1274.
- [8] A.V. Walker, D.A. King, Phys. Rev. Lett. 82 (1999) 5156.
- [9] M.B. Lee, Q.Y. Yang, S.L. Tang, S.T. Ceyer, J. Chem. Phys. 85 (1986) 1693.
- [10] S.T. Ceyer, J.D. Beckerle, M.B. Lee, S.L. Tang, Q.Y. Yang, M.A. Hines, J. Vac. Sci. Technol. A 5 (1987) 501.
- [11] J.D. Beckerle, A.D. Johnson, Q.Y. Yang, S.T. Ceyer, J. Chem. Phys. 91 (1989) 5756.
- [12] P.M. Holmbad, J.H. Larsen, I. Chorkendorff, J. Chem. Phys. 104 (1996) 7289.
- [13] G.R. Schoofs, C.R. Arumanayagam, M.C. McMaster, R.J. Madix, Surf. Sci. 215 (1989) 1.
- [14] A.V. Hamza, R.J. Madix, Surf. Sci. 179 (1987) 25.
- [15] M. Valden, N. Xiang, J. Pere, M. Pessa, Appl. Surf. Sci. 99 (1996) 83.
- [16] M. Valden, J. Pere, N. Xiang, M. Pessa, Chem. Phys. Lett. 257 (1996) 289.
- [17] R.W. Verhoef, D. Kelly, C.B. Mullins, W.H. Weinberg, Surf. Sci. 287 (1993) 94.
- [18] R.W. Verhoef, D. Kelly, C.B. Mullins, W.H. Weinberg, Surf. Sci. 311 (1994) 196.
- [19] R.W. Verhoef, D. Kelly, C.B. Mullins, W.H. Weinberg, Surf. Sci. 325 (1995) 93.
- [20] D.C. Seets, M.C. Wheeler, C.B. Mullins, J. Chem. Phys. 107 (1997) 3986.
- [21] D.C. Seets, C.T. Reeves, B.A. Ferguson, M.C. Wheeler, C.B. Mullins, J. Chem. Phys. 107 (1997) 10229.
- [22] L.B.F. Juurlink, P.R. McCabe, R.R. Smith, C.L. DiCologero, A.L. Utz, Phys. Rev. Lett. 83 (1999) 868.
- [23] A.C. Luntz, J. Harris, Surf. Sci. 258 (1991) 397.
- [24] A.C. Luntz, J. Harris, J. Vac. Sci. Technol. A 10 (1992) 2292.
- [25] A.C. Luntz, J. Chem. Phys. 102 (1995) 8264.
- [26] A.P.J. Jansen, H. Burghgraef, Surf. Sci. 344 (1995) 149.
- [27] M.-N. Carré, B. Jackson, J. Chem. Phys. 108 (1998) 3722.
- [28] H. Yang, J.L. Whitten, J. Chem. Phys. 96 (1992) 5529.
- [29] H. Burghgraef, A.P.J. Jansen, R.A. van Santen, J. Chem. Phys. 98 (1993) 8810.
- [30] H. Burghgraef, A.P.J. Jansen, R.A. van Santen, Chem. Phys. 177 (1993) 407.
- [31] H. Burghgraef, A.P.J. Jansen, R.A. van Santen, J. Chem. Phys. 101 (1994) 11012.
- [32] H. Burghgraef, A.P.J. Jansen, R.A. van Santen, Surf. Sci. 324 (1995) 345.
- [33] P. Kratzer, B. Hammer, J.K. Nørskov, J. Chem. Phys. 105 (1996) 5595.
- [34] C.-T. Au, M.-S. Liao, C.-F. Ng, Chem. Phys. Lett. 267 (1997) 44.
- [35] M.-S. Liao, C.-T. Au, C.-F. Ng, Chem. Phys. Lett. 272 (1997) 445.
- [36] C.-T. Au, C.-F. Ng, M.-S. Liao, J. Catal. 185 (1999) 12.
- [37] H. Bengaard, I. Alstrup, I. Chorkendorff, S. Ullmann, J.R. Rostrup-Nielsen, J.K. Nørskov, J. Catal. 187 (1999) 238.

- [38] R. Milot, A.P.J. Jansen, *J. Chem. Phys.* 109 (1998) 1966.
- [39] U. Manthe, H.-D. Meyer, L.S. Cederbaum, *J. Chem. Phys.* 97 (1992) 3199.
- [40] A.P.J. Jansen, *J. Chem. Phys.* 99 (1993) 4055.
- [41] U. Manthe, H.-D. Meyer, L.S. Cederbaum, *J. Chem. Phys.* 97 (1992) 9062.
- [42] U. Manthe, A.D. Hammerich, *Chem. Phys. Lett.* 211 (1993) 7.
- [43] A.D. Hammerich, U. Manthe, R. Kosloff, H.-D. Meyer, L.S. Cederbaum, *J. Chem. Phys.* 101 (1994) 5623.
- [44] J.-Y. Fang, H. Guo, *J. Chem. Phys.* 101 (1994) 5831.
- [45] J.-Y. Fang, H. Guo, *Chem. Phys. Lett.* 235 (1995) 341.
- [46] J.-Y. Fang, H. Guo, *J. Chem. Phys.* 102 (1995) 1944.
- [47] L. Liu, J.-Y. Fang, H. Guo, *J. Chem. Phys.* 102 (1995) 2404.
- [48] A. Capellini, A.P.J. Jansen, *J. Chem. Phys.* 104 (1996) 3366.
- [49] M. Ehara, H.-D. Meyer, L.S. Cederbaum, *J. Chem. Phys.* 105 (1996) 8865.
- [50] G.A. Worth, H.-D. Meyer, L.S. Cederbaum, *J. Chem. Phys.* 105 (1996) 4412.
- [51] A. Jäckle, H.-D. Meyer, *J. Chem. Phys.* 105 (1996) 6778.
- [52] U. Manthe, F. Matzkies, *Chem. Phys. Lett.* 252 (1996) 71.
- [53] F. Matzkies, U. Manthe, *J. Chem. Phys.* 106 (1997) 2646.
- [54] T. Gerdtts, U. Manthe, *J. Chem. Phys.* 107 (1997) 6584.
- [55] M.H. Beck, H.-D. Meyer, *Z. Phys. D* 42 (1997) 113.
- [56] A. Jäckle, H.-D. Meyer, *J. Chem. Phys.* 109 (1998) 2614.
- [57] A. Jäckle, H.-D. Meyer, *J. Chem. Phys.* 109 (1998) 3772.
- [58] G.A. Worth, H.-D. Meyer, L.S. Cederbaum, *J. Chem. Phys.* 109 (1998) 3518.
- [59] F. Matzkies, U. Manthe, *J. Chem. Phys.* 110 (1999) 88.
- [60] A. Jäckle, M.-C. Heitz, H.-D. Meyer, *J. Chem. Phys.* 110 (1999) 241.
- [61] E.B. Wilson, J.C. Decius, P.C. Cross, *Molecular Vibrations. The Theory of Infrared and Raman Spectra*, McGraw-Hill, London, 1955.
- [62] D.L. Gray, A.G. Robiette, *Mol. Phys.* 37 (1979) 1901.
- [63] T.J. Lee, J.M.L. Martin, P.R. Taylor, *J. Chem. Phys.* 102 (1995) 254.
- [64] H. Burghgraef, A.P.J. Jansen, R.A. van Santen, *Faraday Discuss.* 96 (1993) 337.
- [65] J.C. Light, I.P. Hamilton, J.V. Lill, *J. Chem. Phys.* 82 (1985) 1400.